Alternative Splicing and Caspase-Mediated Cleavage Generate Antagonistic Variants of the Stress Oncoprotein LEDGF/p75

Terry A. Brown-Bryan,[1,2] Lai S. Leoh,[1,2] Vidya Ganapathy,[1,2] Fabio J. Pacheco,[1,6] Melanie Mediavilla-Varela,[1,2] Maria Filippova,[1,3] Thomas A. Linkhart,[5] Rik Gijsbers,[7] Zeger Debyser,[7] and Carlos A. Casiano[1,2,4]

[1]Center for Health Disparities and Molecular Medicine, [2]Division of Microbiology and Molecular Genetics, [3]Division of Biochemistry, and [4]Department of Medicine, Loma Linda University School of Medicine; [5]Muskuloskeletal Disease Center, Jerry L. Pettis Memorial Veterans Affairs Medical Center, Loma Linda, California; [6]Department of Biological Sciences, Centro Universitário Adventista de São Paulo, São Paulo, Brazil; and [7]Molecular Medicine, Katholieke Universiteit Leuven, B-3000, Leuven, Belgium

Abstract

There is increasing evidence that an augmented state of cellular oxidative stress modulates the expression of stress genes implicated in diseases associated with health disparities such as certain cancers and diabetes. Lens epithelium–derived growth factor p75 (LEDGF/p75), also known as DFS70 autoantigen, is emerging as a survival oncoprotein that promotes resistance to oxidative stress–induced cell death and chemotherapy. We previously showed that LEDGF/p75 is targeted by autoantibodies in prostate cancer patients and is overexpressed in prostate tumors, and that its stress survival activity is abrogated during apoptosis. LEDGF/p75 has a COOH-terminally truncated splice variant, p52, whose role in stress survival and apoptosis has not been thoroughly investigated. We observed unbalanced expression of these proteins in a panel of tumor cell lines, with LEDGF/p75 generally expressed at higher levels. During apoptosis, caspase-3 cleaved p52 to generate a p38 fragment that lacked the NH_2-terminal PWWP domain and failed to transactivate the Hsp27 promoter in reporter assays. However, p38 retained chromatin association properties and repressed the transactivation potential of LEDGF/p75. Overexpression of p52 or its variants with truncated PWWP domains in several tumor cell lines induced apoptosis, an activity that was linked to the presence of an intron-derived COOH-terminal sequence. These results implicate the PWWP domain of p52 in transcription function but not in chromatin association and proapoptotic activities. Consistent with their unbalanced expression in tumor cells, LEDGF/p75 and p52 seem to play antagonistic roles in the cellular stress response and could serve as targets for novel antitumor therapies. (Mol Cancer Res 2008;6(8):1293–307)

Introduction

Emerging evidence links the augmented state of cellular oxidative stress with the pathogenesis of diseases associated with health disparities, including cancer and type II diabetes (1-3). Oxidative stress–modulated signaling pathways have been implicated in cancer development and resistance to therapy and may offer attractive targets for therapeutic interventions (4-6). The lens epithelium–derived growth factor p75 (LEDGF/p75), also known as transcription coactivator p75 (TCP75), PC4 and SFRS1 interacting protein (PSIP), and dense fine speckled autoantigen of 70 kDa (DFS70), is emerging as a key player in the cellular response to oxidative stress (7-12). LEDGF/p75 is induced by oxidative stress and is presumed to promote resistance to stress-induced cell death via transcriptional activation of stress and antioxidant genes (8, 9, 13-16). LEDGF/p75 has also been identified as a target of autoantibodies in various autoimmune and inflammatory conditions (17-19) and has emerged as an important cellular cofactor for the chromosomal tethering of HIV-1 (20-24).

A role for LEDGF/p75 in malignancy was first hinted by its homology to members of the hepatoma-derived growth factor family (25) and the observation that chromosomal translocations in leukemias may result in LEDGF/NUP98 fusion

Received 3/6/08; revised 4/20/08; accepted 4/23/08.
Grant support: National Center for Minority Health. and Health Disparities Project EXPORT Program 5P20MD001632/Project 2 (C.A. Casiano), National Institute of Allergy and Infectious Diseases AI44088 (C.A. Casiano), National Institute of General Medical Sciences Initiative for Maximizing Student Diversity 5R25GM60507 (M. Mediavilla-Varela), National Cancer Institute Ruth Kirschstein Minority Predoctoral Fellowship 1F31CA117742-01A1 (M. Mediavilla-Varela), Department of Veterans Affairs Medical Research Merit Review Grant (T. Linkhart), the European Commission LSHB-CT-2003-503480/TRIoH project (R. Gijsbers and Z. Debyser), Basic Research Support Grant from Loma Linda University School of Medicine (C.A. Casiano), and a predoctoral fellowship from Centro Universitario Adventista de Sao Paulo (F.J. Pacheco).
The costs of publication of this article were defrayed in part by the payment of page charges. This article must therefore be hereby marked *advertisement* in accordance with 18 U.S.C. Section 1734 solely to indicate this fact.
Note: T.A. Brown-Bryan and L.S. Leoh contributed equally to this work and share first authorship.
Present address for V. Ganapathy: Department of Medical Oncology, Cancer Institute of New Jersey, New Brunswick, New Jersey. Present address for T.A. Brown-Bryan: Medical Sciences Institute, Charles Drew University of Medicine and Science, Las Angeles, California.
Requests for reprints: Carlos A. Casiano, Center for Health Disparities and Molecular Medicine, Loma Linda University School of Medicine, Mortensen Hall 146, 11085 Campus Street, Loma Linda, CA 92350. Phone: 909-558-1000, ext. 42759; Fax: 909-558-0196. E-mail: ccasiano@llu.edu

doi:10.1158/1541-7786.MCR-08-0125

proteins with potentially altered transcription functions (26-29). We reported that overexpression of LEDGF/p75 in HepG2 liver tumor cells enhanced their proliferation and protected them from stress-induced death (30). We also identified LEDGF/p75 as an autoantigen in prostate cancer whose expression is elevated in advanced stage tumors, most likely as a result of the augmented state of cellular oxidative stress in the prostate tumor microenvironment (31). More recently, Daugaard et al. (32) reported that LEDGF/p75 increases the tumorigenic potential of human cancer cell lines in murine models, and that its expression is increased in human breast and bladder carcinomas. These investigators also provided evidence that overexpression of LEDGF/p75 in HeLa and MCF-7 cells increases chemoresistance. Furthermore, Huang et al. (33) reported increased LEDGF/p75 expression in blasts from chemotherapy-resistant human acute myelocytic leukemia patients.

LEDGF/p75 is composed of 530 amino acids and has an alternative splice variant designated LEDGF/p52 (333 amino acids; hereafter called p52), which also functions as a transcription coactivator of RNA polymerase II and has been implicated in coupling general transcription with mRNA splicing (10, 34, 35). These splice variants share NH_2-terminal amino acids 1 to 325; however, p52 has a unique intron-derived COOH-terminal tail (amino acids 326-333; refs. 10, 34). The NH_2 terminus of both proteins contains a PWWP domain (amino acids 1-93), a highly conserved entity implicated in DNA binding, transcriptional repression, and methylation (30, 36-40). The NH_2 terminus also has three charged domains, a nuclear localization signal and two AT-hook sequences, all important for DNA binding (41, 42). The COOH terminus of LEDGF/p75 has a domain (amino acids 347-429) that shares sequence homology with hepatoma-derived growth factor–related protein 2, and encompasses both the HIV-1 integrase binding domain and the autoepitope recognized by human anti-LEDGF/p75 autoantibodies (30, 43-45). Both the NH_2- and COOH-terminal domains of LEDGF/p75 contribute to its transcription and stress survival functions (30, 33, 46).

Alternative splicing of genes involved in cell death and survival often generates protein isoforms that differ in their domain structure and have antagonistic functions, thus providing regulatory networks that determine the cell fate in response to survival or stress signals (47, 48). Another mechanism for generating protein diversity is the caspase-mediated removal of structural domains in proteins involved in key cellular functions, resulting in the generation of cleavage fragments with dominant-interfering functions that suppress survival pathways and amplify cell death (49). We report here that during apoptosis, caspase-3 removes the PWWP domain of p52 to generate a p38 fragment that interferes with the transactivation potential of LEDGF/p75. Disruption of this domain inhibits the transcriptional function of p52 but not its interaction with chromatin. We also observed that transient overexpression of p52 in various tumor cell lines induced apoptosis, and that this activity was independent of the PWWP domain. These studies provide initial clues for a mechanistic understanding of how alternative splicing and caspase-mediated cleavage of LEDGF modulate tumor cell survival and death under stress.

Results

Unbalanced Intracellular Expression of LEDGF/p75 and p52

Elevated LEDGF/p75 protein levels have been detected in various cancer cell lines (31-33); however, the relative protein expression levels of LEDGF/p75 and p52 in tumor cells have not been analyzed. Immunoblotting analysis with a monoclonal antibody directed against the common NH_2-terminal domain revealed unbalanced expression of these splice isoforms in various tumor and nontumor cell lines, with p52 protein levels generally lower than those of LEDGF/p75 (Fig. 1). The highest p52 levels were observed in the HCT116, U2OS, and 22Rv1 cell lines, which also had relatively high LEDGF/p75 expression. Cell lines with relatively low LEDGF/p75 expression (e.g., HepG2, PrEC, and PrSC) displayed negligible p52 protein levels.

LEDGF/p52 Is Cleaved by Effector Caspases at the PWWP Domain

We previously showed that caspase-3 disrupts the NH_2-terminal PWWP and COOH-terminal domains of LEDGF/p75, abrogating its ability to protect against stress-induced cell death (30). Because LEDGF/p75 and p52 share identical PWWP domains, we hypothesized that the cellular functions of p52 may also be modulated by caspases during apoptosis. Cleavage of p52 into a 38-kDa fragment (hereafter called p38) was detected in various human tumor cell lines undergoing apoptosis (Fig. 2A and B) and coincided with increased caspase-3/7 activity (Fig. 2C). The caspase dependency of this cleavage was confirmed by its inhibition with the pan-caspase inhibitor benzylozycarbonyl-Val-Ala-Asp-fluoromethylketone (z-VAD-fmk) and the caspase-3/7 inhibitor benzylozycarbonyl-Asp-Glu-Val-Asp-fluoromethylketone (z-DEVD-fmk; Fig. 2D).

To investigate the mechanism of apoptotic p52 cleavage, *in vitro* translated p52 fused to a hemagglutinin (HA) tag was incubated with individual recombinant caspases. Caspase-3 and caspase-7, but not caspase-6, caspase-8, and caspase-9, cleaved HA-p52 into p48 and p38 fragments, although caspase-7 seemed to be less efficient in generating p38 (Fig. 3A). LEDGF/p75, which we previously established as a substrate of caspase-3 and caspase-7 but not of caspase-6 (28), was used in control experiments (Fig. 3A). Caspase activity assays indicated that each recombinant caspase was active (data not shown). Caspase-3 cleaved HA-p52 sequentially into p48 and p38 in a dose- and time-dependent manner (Fig. 3B). The p48 fragment could be distinguished from HA-p52 *in vitro* but was not consistently resolved from endogenous p52 in apoptotic cells (Fig. 2). Based on the known caspase cleavage sites in the PWWP domain of LEDGF/p75 (30), we identified two candidate cleavage sites in the p52 PWWP domain, $DEVPD^{30}$ and $WEID^{85}$, which would generate p48 and p38 (Fig. 3C). To map these sites, we substituted aspartic acids at positions 30 and 85 in HA-p52 with alanines to generate partial caspase-resistant mutants, HA-DEVPA and HA-WEIA, and a complete caspase-resistant double mutant, HA-DM. The mutations were confirmed by DNA sequencing. *In vitro* cleavage of HA-DEVPA by caspase-3 generated p38, consistent with cleavage at the available $WEID^{85}$ site. Cleavage of HA-WEIA generated p48, consistent with cleavage at the available $DEVPD^{30}$ site (Fig. 3D). Incubation of

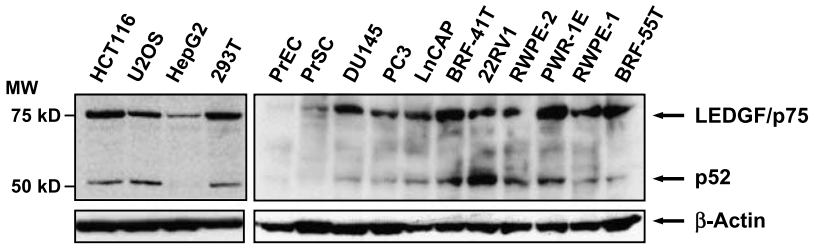

FIGURE 1. Immunoblotting analysis of endogenous protein expression of LEDGF/p75 and p52 in a panel of human normal and cancer cell lines. Cell lines used were HCT116 (colon carcinoma), U2OS (osteosarcoma), HepG2 (hepatocarcinoma), 293T (embryonic kidney), PrEC (normal prostate epithelium), PrSC (normal prostate stroma), DU145 (prostate carcinoma), PC3 (prostate adenocarcinoma), LnCAP (prostate carcinoma), BRF-41T (prostate adenocarcinoma), 22RV1 (prostate carcinoma), RWPE-2 (transformed normal prostate epithelial cell line, tumorigenic), PWR-1E (transformed normal epithelial cell line, nontumorigenic), RWPE-1 (transformed normal epithelial cell line, nontumorigenic), and BRF-55T (benign prostatic hyperplasia). Proteins in whole-cell lysates were separated by SDS-PAGE, transferred to nitrocellulose, and detected by chemiluminescence with a monoclonal antibody that recognizes both LEDGF/p75 and p52. Monoclonal antibody to β-actin was used as a loading control.

HA-DM with caspase-3 failed to generate p48 and p38, consistent with blockade of both cleavage sites.

For further exploration of the cleavage sites and subsequent experiments, we generated HA-tagged truncated variants of p52 corresponding to p48 and p38 by deleting amino acids 1 to 30 (HA-DN30) and 1 to 85 (HA-DN85), respectively. The deletions were confirmed by DNA sequencing. *In vitro* translated HA-p52 migrated slightly slower than endogenous p52 due to the presence of the tag (Fig. 3E, compare *lanes 1* and *3*); however, its cleavage by caspase-3 generated the p48 and p38 fragments (Fig. 3E, compare *lanes 2* and *4*). *In vitro* translated HA-DN30 and HA-DN85 also displayed slightly slower electrophoretic migration than their corresponding cleavage fragments p48 and p38 (Fig. 3E, compare *lane 4* with *lanes 5* and *7*). However, incubation of HA-DN30 with caspase-3 generated fragments that corresponded to p48 and p38 (Fig. 3E, compare *lanes 4* and *6*), suggesting that this protease cleaved the HA tag to produce p48 and then removed most of the PWWP domain to produce p38. Likewise, incubation of HA-DN85 with caspase-3 generated a slightly faster migrating fragment corresponding to p38 (Fig. 3E, compare *lanes 4* and *8*), again consistent with cleavage of the HA tag. A parallel experiment in which the blots were incubated with an anti-HA antibody revealed loss of HA tag immunoreactivity in the HA-tagged proteins incubated with caspase-3 (Fig. 3F).

Disruption of the PWWP Domain Abrogates p52 Transactivation Potential

Based on previous observations that the NH_2 terminus of LEDGF/p75 (amino acids 1-187) transactivates the Hsp27 promoter (*Hsp27pr*) by binding to stress-response elements (STRE) present in this promoter (46), we predicted that p52 would also transactivate this promoter in transient transfection assays with a luciferase (Luc) reporter construct. This system was used to examine the effect of caspase-mediated disruption of the PWWP domain on p52 transactivation potential. A schematic representation of the p52 constructs used in the reporter assays is depicted in Fig. 4A. The electrophoretic migration of the *in vitro* translated constructs is shown in Fig. 4B. Colorectal carcinoma HCT116 cells were transiently cotransfected with the pGL3 basic plasmid, with or without a proximal *Hsp27pr*, and effector pCruz plasmids encoding HA-LEDGF/p75 or HA-p52. Both fusion proteins showed significant induction of Luc activity ($P < 0.05$) as well as comparable expression levels (Fig. 4C). Similar results were obtained in U2OS osteosarcoma cells (data not shown). The induction of endogenous Hsp27 mRNA by ectopically expressed HA-LEDGFp75 and HA-p52 was confirmed by reverse transcription-PCR (Fig. 4D).

Next, we analyzed the transactivation potential of the cleavage fragments (p48/HA-DN30 and p38/HA-DN85) and the caspase-resistant mutants (HA-DEVPA, HA-WEIA, and HA-DM). P48/HA-DN30 and p38/HA-DN85 did not increase *Hsp27pr*-Luc activity above the basal level observed in empty pCruz vector–transfected cells, whereas the caspase-resistant mutants (all of which had an intact PWWP domain) were as effective as HA-p52 in transactivating the promoter (Fig. 4E). Other PWWP deletion constructs of p52 (i.e., HA-DN18, HA-DN18M, HA-DN26, HA-DN50, and HA-DN100) also showed decreased transactivation potential (Fig. 4F). HA-DN18M, which contains a tryptophan[21] to alanine[21] mutation in the PHWP motif (amino acids 19-22), the most conserved sequence within the PWWP domain (30), showed slightly less activity than HA-DN18, but the mean difference was not significant.

p38 Interferes with the Transactivation Potential of LEDGF/p75

The p38/HA-DN85 fragment seemed to be relatively stable in apoptotic cells and lacked the ability to transactivate *Hsp27pr*-Luc (Figs. 2-4). To determine whether this fragment might possess transcription repression properties, we examined its influence on the transactivation potential of LEDGF/p75 and p52. The p38/HA-DN85 construct was cotransfected in HCT116 cells with either HA-LEDGF/p75 or HA-p52 in the presence of the luciferase reporter plasmids. P38/HA-DN85 significantly repressed the transactivation potential of HA-LEDGF/p75 ($P < 0.05$) but not that of HA-p52 (Fig. 5A). Although the p38/HA-DN85 construct was transfected at submaximal doses, it seemed to be highly stable because its protein expression was consistently higher than those of LEDGF/p75 and p52 (Fig. 5B).

To determine if p38/HA-DN85 colocalized with both LEDGF/p75 and p52 in the chromatin, we examined their nuclear localization in U2OS cells. Nuclei from cells expressing

HcRed-p52 and p38/HA-DN85 displayed chromatin condensation and margination, whereas nuclei from cells expressing HcRed-p75 displayed normal morphology (Fig. 5C). Consistent with its repression activity, p38/HA-DN85 colocalized with both HcRed-LEDGF/p75 and HcRed-p52 in the chromatin (Fig. 5D).

The PWWP Domain of p52 Is Dispensable for Chromatin Association

The colocalization of p38/HA-DN85 with chromatin, despite lacking most of the PWWP domain (Fig. 5), suggested that this domain might not be essential for the association of p52 with chromatin. To confirm this, the intracellular expression of the HA-p52 and its PWWP deletion mutants was examined by immunofluorescence microscopy. All the HA-p52 variants showed nuclear distribution and colocalized with chromatin, despite some of them having truncated PWWP domains (Fig. 6A). To biochemically support this observation, we extracted soluble, nuclear, and chromatin fractions from cells overexpressing HA-p52 or its deletion mutants and examined them by immunoblotting the distribution of the individual proteins in the different fractions. HA-LEDGF/p75, HA-p52, and HA-DM were found predominantly in the chromatin fraction (Fig. 6B). However, as increasing segments of the PWWP domain were deleted from p52, a portion of the truncated proteins accumulated in the soluble fractions (Fig. 6B), suggesting that the PWWP domain may contribute but is not essential to chromatin association.

Transient Overexpression of p52 Induces Caspase-Dependent Apoptosis

We noticed that many U2OS cells transiently overexpressing HA-p52, HA-DM, p38/HA-DN85, or the other PWWP-truncated mutants displayed characteristic features of apoptosis such as nuclear margination and partial nuclear fragmentation (Fig. 6A). By contrast, most cells transfected with empty pCruz vector or overexpressing HA-LEDGF/p75 showed normal nuclear morphology. The nuclear apoptotic-like morphology was more pronounced in cells transiently overexpressing HcRed-p52, which exhibited rounding; detachment; and considerable nuclear condensation, margination, and fragmentation (Fig. 7A). Approximately 80% of U2OS cells ectopically expressing HcRed-p52 displayed an apoptotic-like nuclear

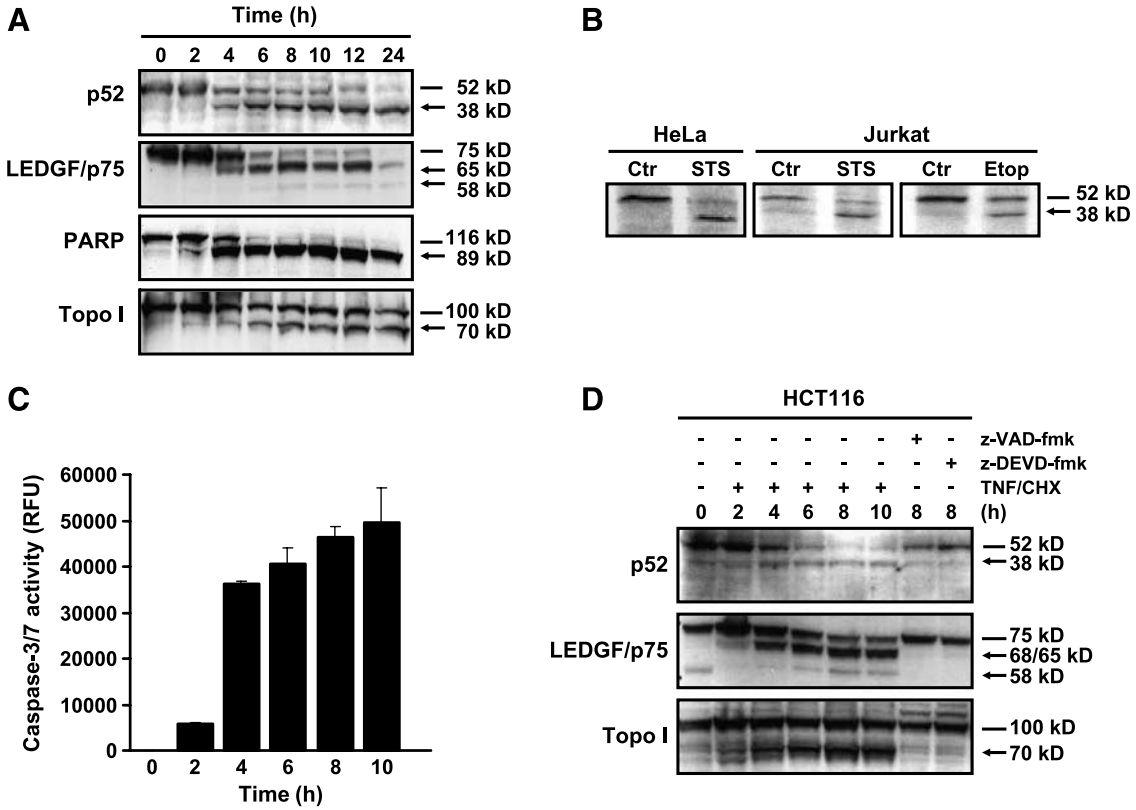

FIGURE 2. Caspase-mediated cleavage of p52 during apoptosis. **A.** Immunoblotting analysis of p52 cleavage in apoptotic HCT116 cells. Apoptosis was induced by treatment with TNF-α (10 ng/mL) in combination with 20 μmol/L cycloheximide for the indicated times. Proteins were detected by immunoblotting with rabbit affinity-purified polyclonal anti-p52, human anti-LEDGF/p75, and anti–topoisomerase I (*Topo I*) autoantibodies and mouse monoclonal anti–poly(ADP-ribose) polymerase (*PARP*). **B.** Immunoblotting analysis of p52 cleavage in apoptotic HeLa and Jurkat cells. Apoptosis was induced by treatment with 2 μmol/L staurosporine (*STS*) or 150 μmol/L etoposide (*Etop*) for 6 h. **C.** Caspase-3/7 activity in TNF-α/cycloheximide–treated HCT116 cells. Activity was determined by cleavage of the fluorogenic substrate DEVD-AMC and expressed in relative fluorescence units (*RFU*), from which the value of the untreated control was subtracted. Columns, mean of three independent experiments done in triplicate; bars, SD. **D.** HCT116 cells were treated with TNF-α/cycloheximide for up to 10 h, with and without 1-h preincubation with 100 μmol/L of z-VAD-fmk or the caspase-3/7 inhibitor z-DEVD-fmk. Lysates were analyzed by immunoblotting with rabbit anti-p52 and human anti-LEDGF/p75 and anti–topoisomerase I antibodies. Lines, intact proteins; arrows, cleavage fragments.

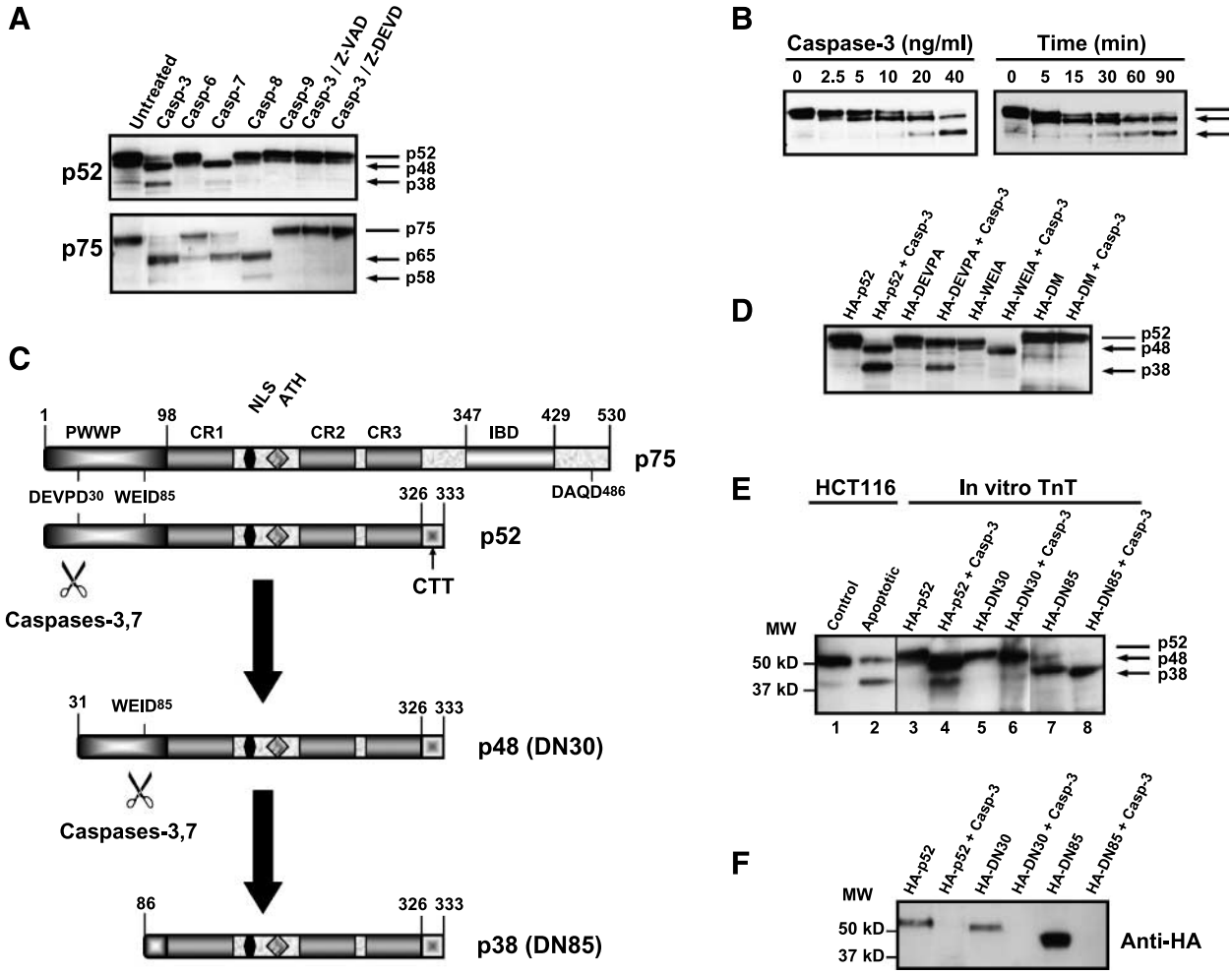

FIGURE 3. Caspase-3 and caspase-7 cleave p52 at two sites *in vitro* to generate p48 and p38 fragments. **A.** *In vitro* translated biotinylated HA-p52 was incubated with 20 ng/mL of purified recombinant caspase-3, caspase-6, caspase-7, caspase-8, and caspase-9 for 2 h. HA-LEDGF/p75 was included as a positive control. Some experiments were done in the presence or absence of 10 μmol/L z-VAD-fmk or z-DEVD-fmk. Translated biotinylated proteins were separated by SDS-PAGE, transferred to nitrocellulose, and detected with HRP-streptavidin and enhanced chemiluminescence. **B.** *In vitro* translated biotinylated HA-p52 was treated with increasing concentrations of caspase-3 or with 20 ng/mL caspase-3 for the indicated times and analyzed as described above. **C.** Schematic representation of LEDGF/p75 and p52 showing their domain structure, the location of the putative caspase cleavage sites ($DEVD^{30}$ and $WEID^{85}$), and the p52 cleavage fragments (p48/DN30 and p38/DN85). CR, charged region; NLS, nuclear localization region, ATH, AT-hooks; IBD, integrase binding domain; CTT, COOH-terminal tail. **D.** *In vitro* translated HA-p52 and its mutants HA-DEVPA, HA-WEIA, and HA-DM were exposed to recombinant caspase-3 for 2 h and analyzed as described above. **E.** Comparison of the migration in SDS-PAGE of endogenous p52 and its cleavage products derived from control and apoptotic HCT116 cells (*lanes 1* and *2*) with the migration of intact and caspase-3 cleaved HA-p52 (*lanes 3* and *4*), HA-DN30 (*lanes 5* and *6*), and HA-DN85 (*lanes 7* and *8*). Lanes 1 and 2, endogenous proteins detected by immunoblotting with anti-p52 antibody; lanes 3 to 8, translated biotinylated proteins detected in blots with HRP-streptavidin. Lanes 1 to 6 are from the same blot, whereas lanes 7 and 8 are from a blot done in parallel under identical conditions. **F.** Immunoblot, using an anti-HA antibody, of translated HA-tagged proteins incubated with and without caspase-3.

morphology, compared with 12% of cells expressing HcRed-LEDGF/p75 or 10% of cells transfected with empty pHcRed C1 vector ($P < 0.001$; Fig. 7B). In the total cell population, ~27% of cells transfected with pHcRed-p52 exhibited a nuclear apoptotic morphology, compared with 6% of total cells transfected with pHcRed-p75. Transfection efficiency, measured by the number of cells expressing the HcRed fusion proteins, was ~30% using the Fugene 6 reagent, which was the method of choice for these experiments due to its minimal cytotoxicity (50). These results were reproduced in HCT116 and HeLa cells (data not shown).

Cell survival, measured by reduction of 3-(4,5-dimethylthiazol-2-yl)-2,5-diphenyltetrazolium bromide, was significantly reduced in the total U2OS cell population transfected with pHcRed-p52, compared with cells transfected with empty pHcRed-C1 vector or pHcRed-LEDGF/p75 ($P < 0.05$; Fig. 7C). This reduction was reversed by z-VAD-fmk (Fig. 7C), suggesting that pHcRed-p52–induced apoptosis was caspase dependent. Comparable results were obtained in control cells overexpressing the proapoptotic protein Bad (Fig. 7C). To further confirm that HcRed-p52–induced cell death was caspase dependent, we measured caspase activation in U2OS cells transiently transfected with HcRed-p52. Significant activation of caspase-3, caspase-8, and caspase-9 and abolition of caspase activity by z-VAD-fmk were observed (Fig. 8A). Furthermore, immunoblotting of U2OS whole-cell lysates expressing

HcRed-p52 showed cleavage of poly(ADP-ribose) polymerase and lamin B into their signature 46-kDa and 89-kDa apoptotic fragments, respectively, as well as caspase-3 and caspase-8 processing into their active 17- to 15-kDa and 18-kDa fragments, respectively (Fig. 8B). There was also an increase in the amount of HcRed protein, likely resulting from its removal from p52 by caspase-3 cleavage at the PWWP domain (Fig. 8B). HcRed-p52–induced caspase processing and activation and nuclear substrate

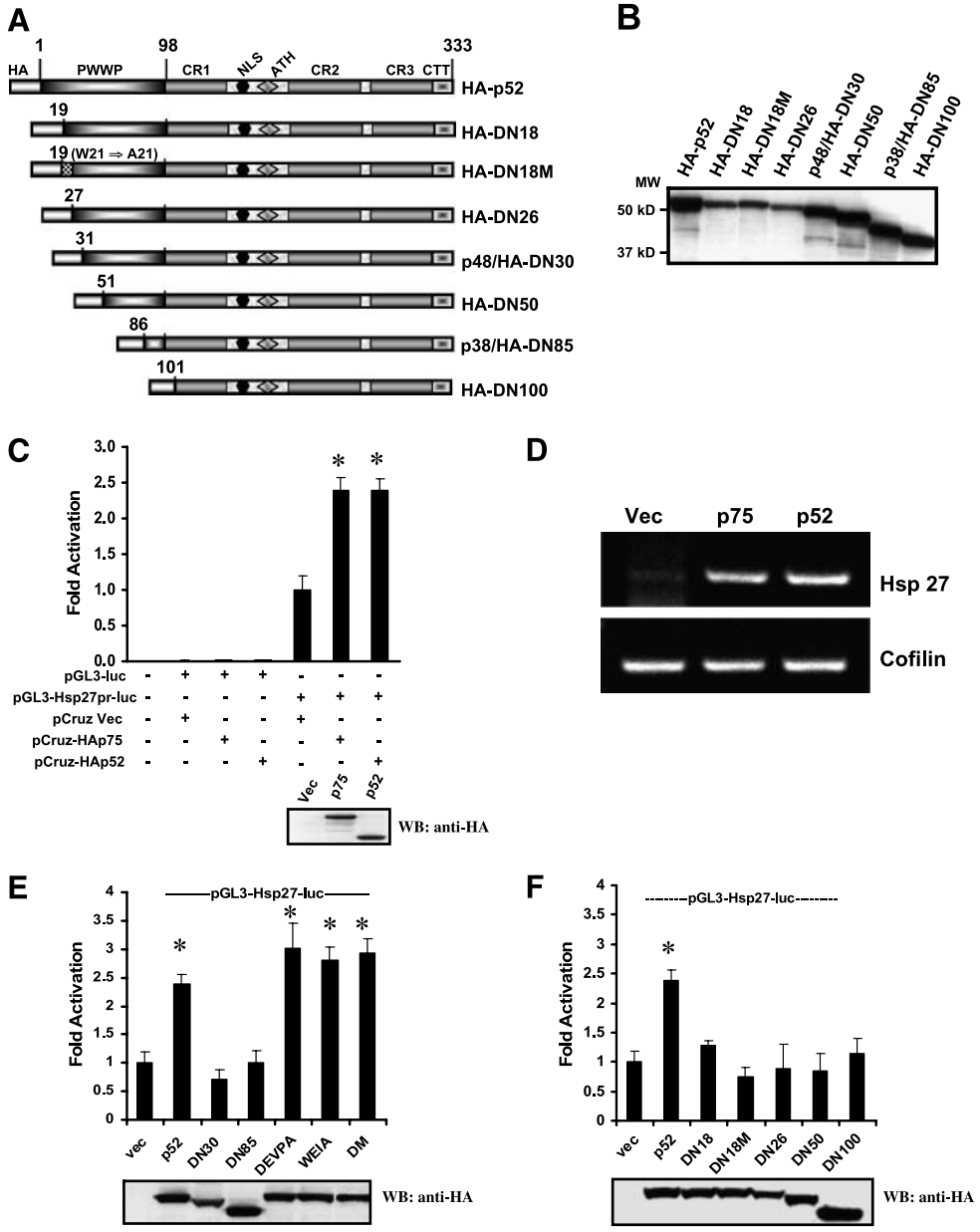

FIGURE 4. Caspase-mediated disruption of the PWWP domain of p52 abrogates its transcriptional potential. **A.** Schematic representations of HA-p52 and its PWWP deletion constructs used in luciferase-based reporter assays. The numbered DN constructs indicate the total amino acids deleted from the NH_2 terminus of p52. Numbers above the constructs indicate amino acid positions. **B.** HA-p52 and its PWWP deletion constructs were *in vitro* translated and biotinylated, separated by SDS-PAGE, transferred to nitrocellulose, and detected with HRP-streptavidin and enhanced chemiluminescence. **C.** HCT116 cells were cotransfected with pCruzHA (empty vector or encoding LEDGF/p75 or p52) and pGL3 luciferase reporter vector (with or without the Hsp27 promoter region) and cultured for 48 h. Cells were then lysed and assayed to determine luciferase activity or analyzed by immunoblotting with rabbit anti-HA antibody. **D.** HCT116 cells were transfected with pCruzHA (empty vector or encoding LEDGF/p75 or p52) and reverse transcription-PCR analysis was carried out after 48 h using a PCR primer pair specific for the human *HSP27* gene. The *Cofilin* gene was amplified as a control. **E.** HCT116 cells were cotransfected with pCruzHA (empty vector or encoding p52, its caspase cleavage fragments p48/DN30 and p38/DN85, or its cleavage resistant mutants DEVPA, WEIA, and DM) and pGL3 luciferase reporter vector with the Hsp27 promoter region and assayed for luciferase activity and immunoblotting. **F.** HCT116 cells were cotransfected with pCruzHA (empty vector or encoding p52 and its PWWP deletion mutant DN18, DN18M, DN26, DN50, or DN100) and pGL3 luciferase reporter vector with the Hsp27 promoter region and assayed for luciferase activity and immunoblotting. Fold activation of luciferase activity was determined as described in Materials and Methods. Corresponding Western blots showing the expression of the different HA fusion proteins after 48-h transfection are included in **C**, **E**, and **F**. Columns, mean of three independent experiments done in triplicate; bars, SD. *, $P < 0.05$, compared with fold activation generated by cotransfection of pGL3-*Hsp27pr*-Luc and empty pCruz vector (one-way ANOVA, GraphPad Prism).

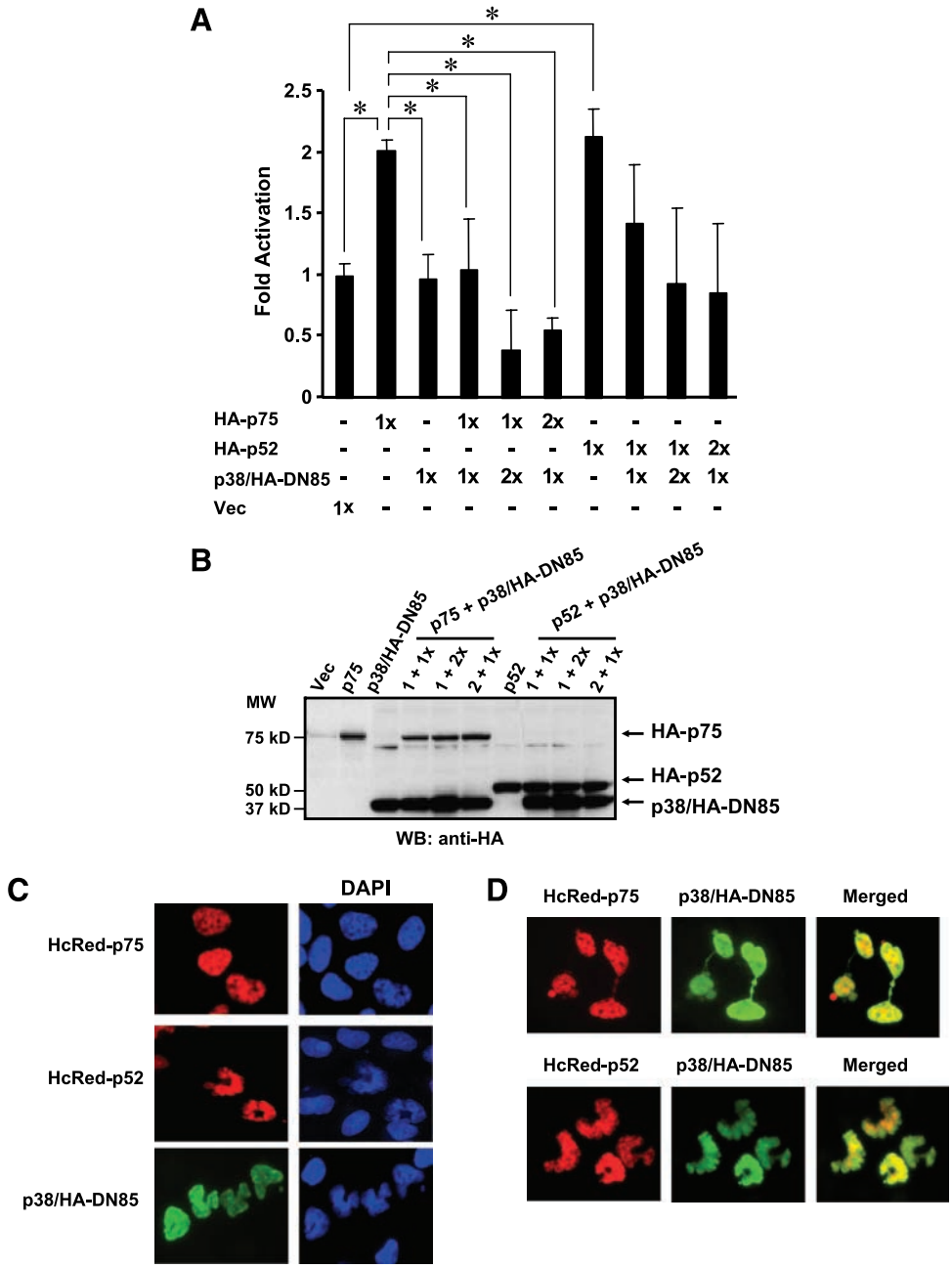

FIGURE 5. The p38 cleavage fragment interferes with the transactivation potential of LEDGF/p75. **A.** Either 1 μg (1×) or 2 μg (2×) of pCruzHA-LEDGF/p75 or pCruzHA-p52 DNA were cotransfected with 0.2 μg (1×) or 0.4 μg (2×) of pCruzHA-DN85 or empty vector (*Vec*), together with the pGL3-*Hsp27pr*-Luc reporter plasmid. HCT116 cells were lysed after 48 h and assayed for fold induction of luciferase activity. Columns, mean of three independent experiments done in quadruplicate; bars, SD. *, $P < 0.05$, one-way ANOVA with Bonferroni's multiple comparison test (GraphPad Prism). **B.** Corresponding immunoblot showing recombinant protein expression, detected with anti-HA antibody, 48 h after transfection in HCT116 cells. **C.** U2OS cells were transiently transfected with pHcRed-LEDGF/p75, pHcRed-p52, or pCruzHA-p38/DN85 and then grown in coverslips. After 48 h, recombinant protein expression in transfected cells was visualized by fluorescence microscopy. After fixation and permeabilization, HcRed-LEDGF/p75 and HcRed-p52 were visualized directly, whereas HA-p38/DN85 was detected with primary rabbit anti-HA antibody with secondary Alexa 488–labeled goat anti-rabbit antibody. Nuclei were counterstained with 4′,6-diamidino-2-phenylindole (*DAPI*). **D.** Cells were cotransfected with pCruzHA-p38/DN85 (0.5 μg) and pHcRed-LEDGF/p75 (1 μg) or pHcRed-p52 (1 μg), stained with anti-HA antibodies, and visualized by fluorescence microscopy.

cleavage were not as dramatic as those triggered by overexpression of p53 or treatment with tumor necrosis factor (TNF) or staurosporine (Fig. 8A and B). This might be due to the relatively low transfection efficiency (<30%) attained when using pHcRed plasmids. Lamin B and poly(ADP-ribose) polymerase cleavages were not observed in cells transfected with empty pHcRed vector or pHcRed-LEDGF/p75 (Fig. 8C).

The COOH-Terminal Tail Contributes to p52 Apoptotic Activity but not to Its Transactivation Potential

The observation that transient overexpression of p52 and its PWWP-truncated variants induced a nuclear apoptotic morphology suggested that the PWWP domain is dispensable for proapoptotic activity. However, because all the p52 constructs retained the intron-derived COOH-terminal tail, we investigated whether this sequence might contribute to proapoptotic activity and transactivation potential. For these experiments, we generated an HcRed-p52DC construct lacking the COOH-terminal tail (Fig. 9A). We observed that HcRed-p52DC transactivated *Hsp27pr*-Luc at levels comparable with those of HcRed-p52 and HcRed-LEDGF/p75 ($P < 0.05$; Fig. 9B), suggesting that the COOH-terminal tail is not required for transactivation potential. To determine if the COOH-terminal tail is required for proapoptotic activity, we counted nuclei with

highly condensed, fragmented, or marginated chromatin in U2OS and prostate adenocarcinoma cell lines transiently transfected with empty pHcRed-C1 vector, pHcRed-LEDGF/p75, pHcRed-p52, or pHcRed-p52DC. Consistent with the results presented in Fig. 7, ~80% of U2OS cells expressing HcRed-p52 displayed an apoptotic-like nuclear morphology ($P < 0.001$; Fig. 9C). In contrast, ~30% of cells expressing HcRed-p52DC and <20% of cells transfected with empty vector or pHcRed-LEDGF/p75 displayed a nuclear apoptotic morphology ($P < 0.05$). Comparable results were obtained in the prostate cancer cell lines PC3 and 22rv1, although the percentage of apoptotic nuclei was between 50% and 60% (Fig. 9D and data not shown). These results suggested differential sensitivity to the proapoptotic activity of transiently overexpressed p52 among various cell lines, and that the COOH-terminal tail might contribute to this activity.

Discussion

This study was undertaken as part of our efforts to delineate mechanisms by which alternative splicing and caspase cleavage of LEDGF modulate tumor cell death and survival under stress. Our data suggest that p52, a short splice variant of LEDGF/p75, is cleaved during apoptosis by caspase-3 at the DEVPD[30] site to generate a p48 fragment, which is subsequently cleaved at the WEID[85] site to generate a stable p38 fragment lacking the PWWP domain. The p48 fragment did not seem to accumulate in apoptotic cells, perhaps due to its rapid cleavage into p38 or the inaccessibility of the DEVPD[30] site to caspases *in vivo*. Alternatively, our electrophoretic conditions were not conducive to optimal resolution of endogenous p52 from p48.

The DEVPD[30] and WEID[85] cleavage sites are conserved in the PWWP domains of LEDGF/p75 and p52 but absent in other PWWP-containing proteins (30). Disruption of the PWWP domain abrogated the ability of p52 to transactivate *Hsp27pr* in reporter assays, suggesting that this domain is essential for p52 transcription function. By contrast, Singh et al. (46) reported that deletion of NH_2-terminal amino acids 1 to 198 of LEDGF/p75 significantly enhanced transactivation of *Hsp27pr*, suggesting that the PWWP domain of this protein may have transcription repression function. Consistent with this report, we observed that truncation of the PWWP domain of LEDGF/p75 increased transactivation of *Hsp27pr* (51). It should be noted that NUP98-LEDGF fusion proteins involving both p75 and p52, which result from chromosomal translocations in leukemias, lack the PWWP domain because the fusion point is at amino acid position 153 (26, 33). This would result in transcriptionally hyperactive NUP98-p75 but transcriptionally inactive NUP98-p52, potentially providing a survival advantage to leukemic cells. Interestingly, the PWWP domain of the histone methyltransferase WHISTLE was recently implicated in its transcription repression and proapoptotic activities (52). Our data suggest that the p52 PWWP domain is required for transcription function, although we cannot rule out that it may be involved in transcriptional repression.

Our results also suggested that the PWWP domain of p52 is dispensable for chromatin association. Although this would be consistent with reports indicating that the association of LEDGF/p75 with chromatin is mediated primarily by structural elements downstream of the PWWP domain, particularly AT-hooks (41, 42), a recent study revealed that this domain is required for LEDGF/p75 binding to nucleosomes *in vitro* (53).

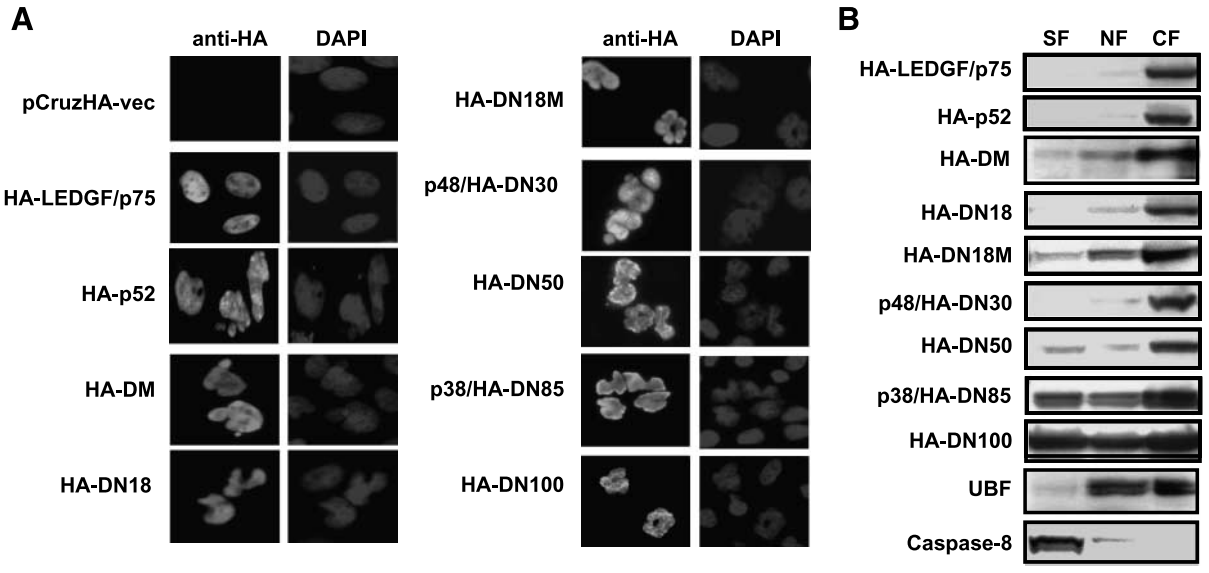

FIGURE 6. Effect of PWWP domain disruption on the chromatin association properties of p52. **A.** U2OS cells were transiently transfected with pCruz plasmid encoding HA-LEDGF/p75, HA-p52, or the p52 variants with a truncated PWWP domain. After 48 h, the expressed HA-tagged proteins were visualized by fluorescence microscopy as indicated in the legend of Fig. 5. Nuclei were counterstained with 4′,6-diamidino-2-phenylindole (DAPI). Images are representative of at least two experiments. **B.** Immunoblotting analysis of soluble (*SF*), nuclear (*NF*), and chromatin (*CF*) fractions of HCT116 cells transiently expressing HA-LEDGF/p75, HA-p52, or the p52 variant with a truncated PWWP domain. Proteins in the different fractions were separated by SDS-PAGE, transferred to nitrocellulose, and detected with anti-HA antibody. The relative purity of each fraction was evaluated by immunoblotting with antibodies to caspase-8 (soluble fraction), upstream binding factor (*UBF*; present in both nuclear fraction and chromatin fraction), and LEDGF/p75 (chromatin fraction).

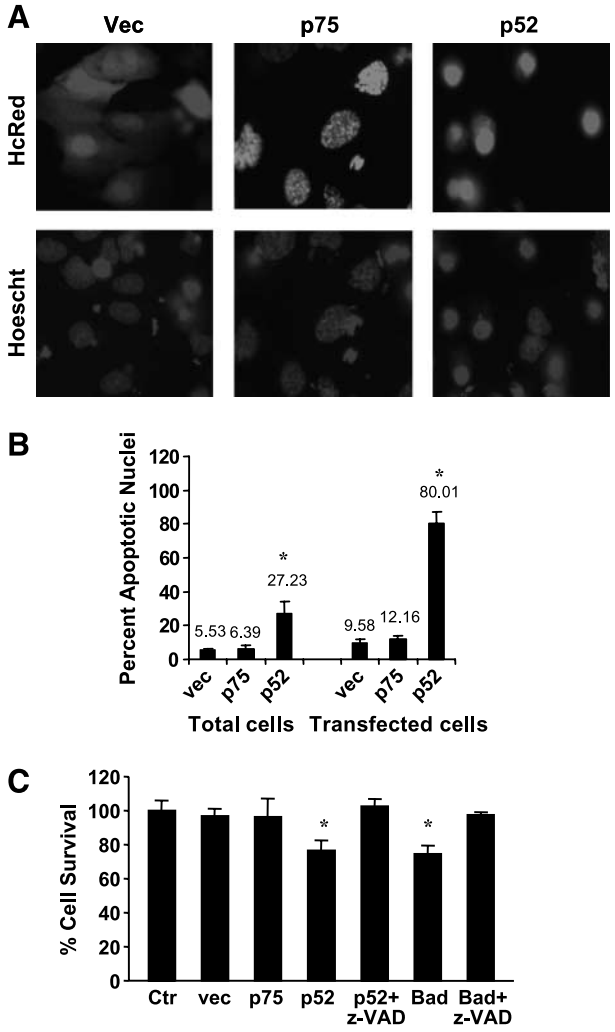

FIGURE 7. Ectopic expression of p52, but not LEDGF/p75, induces features of apoptotic cell death. **A.** U2OS cells were transiently transfected with pHcRed-LEDGF/p75, pHcRed-p52, or empty pHcRed vector. Forty-eight hours posttransfection, nuclei were counterstained with Hoechst and cells were visualized by fluorescence microscopy. **B.** The percent of apoptotic nuclei was calculated for both the total and transfected cell populations based on the number of cells with nuclei exhibiting marked chromatin margination, fragmentation, or condensation. **C.** Percentage of surviving cells transiently expressing p52. U2OS cells were transfected as in **A**. An additional plasmid encoding the proapoptotic protein Bad (pcDNA-FLAG-Bad) was used as a positive control for cell death induction. Cells were also pretreated for 1 h with the pancaspase inhibitor z-VAD-fmk before transfection with pHcRed-p52 and pcDNA-FLAG-Bad. Forty-eight hours posttransfection, cell survival was determined with the 3-(4,5-dimethylthiazol-2-yl)-2,5-diphenyltetrazolium bromide assay. The 450-nm absorbance values were normalized to the values for untransfected cells, which were assumed to be 100% viable. Columns, mean of three independent experiments done in triplicate; bars, SD. *, $P < 0.05$, compared with empty pHcRed vector (one-way ANOVA, GraphPad Prism).

Retention of AT-hooks in p38 may facilitate its association with chromatin, where it might act as a specific transcription repressor, conceivably by competing with LEDGF/p75 for chromatin binding sites or preventing its interactions with specific transcription factors. This would be consistent with evidence that caspase-mediated cleavage of certain transcription factors generates dominant-interfering fragments with DNA-binding activities but lacking transactivation potential (54-56).

Whereas LEDGF/p75 is known to transactivate specific stress genes (9, 13-16), the target genes of p52 are unknown. We observed that ectopic expression of p52 induced *Hsp27* mRNA expression and transactivated *Hsp27pr*-Luc, most likely through binding of its NH_2-terminal portion (amino acids 1-187) to STRE in this promoter, as reported for LEDGF/p75 (46). Preliminary gel shift assays using nuclear extracts indicated binding of both p75 and p52 to STRE consensus sequences (A/TGGGG/T) in *Hsp27pr*, but these results await to be confirmed by supershift assays and other additional carefully controlled experiments (data not shown). It should be emphasized that if additional experiments confirm a role for the PWWP domain in consensus sequence binding, this would not be a major contributor to p52 chromatin binding function. It remains to be established whether *Hsp27* is a true target gene of p52 or its transactivation by p52 is an indirect or relatively nonspecific event that occurs within the context of general mRNA transcription. It is also plausible that p52-induced caspase-3 activation might lead to disruption of the PWWP domain of LEDGF/p75 by cleavage at the $DEVPD^{30}$ site (30), resulting in enhanced *Hsp27pr* transactivation by PWWP-truncated LEDGF/p75 (46, 51).

The transient overexpression of p52 and its PWWP-truncated mutants induced features of apoptosis in U2OS and other cell lines. Whereas cells overexpressing HA-p52 exhibited chromatin margination with moderate nuclear fragmentation, cells expressing HcRed-p52 exhibited a pronounced nuclear apoptotic morphology. A possible explanation for these differences could be that the HA tag was removed from p52 early during apoptosis by caspase cleavage at the $DEVPD^{30}$ site, preventing the visualization of HA-p52–stained nuclei with pronounced apoptotic morphology. During apoptosis, the HA tag is cleaved by caspases, resulting in the loss of immunoreactivity (57). This would be consistent with the results shown in Fig. 3E and F.

A previous study showed that cells overexpressing green fluorescent protein (GFP)-p52 displayed intense nuclear fluorescence, rough or deformed nuclear morphology, multiple small nuclei, and loss from the cell population in culture (58). These features are consistent with apoptotic cell death. By contrast, cells overexpressing GFP-p75 survived well and displayed normal nuclear morphology (58), consistent with our results. It cannot be ruled out, however, that the presence of a tag (HA, HcRed, or GFP) induces p52, but not LEDGF/p75, to behave as a proapoptotic protein. During the preparation of this article, Huang et al. (33) reported up-regulation of both LEDGF/p75 and p52 in chemoresistant acute myelocytic leukemia blasts, with LEDGF/p75 being the most consistently up-regulated mRNA. Interestingly, these investigators identified splice variants of p52 displaying proapoptotic and antiapoptotic effects. However, they did not examine the proapoptotic or antiapoptotic effects of the p52 isoform (amino acids 1-333) used in our study.

The proapoptotic effects of overexpressed p52 seem to be independent of its transcriptional activity, given that ectopic expression of p38/HA-DN85 and other PWWP

deletion mutants also induced apoptotic nuclear morphology. It cannot be ruled out, however, that under stress conditions p52 might transactivate proapoptotic genes or repress survival genes, leading to caspase activation and consequently inducing its own cleavage, as well as that of LEDGF/p75, into proapoptotic dominant-interfering fragments that amplify the cell death process. This would be consistent with our previous observation that stable overexpression of a p65 caspase cleavage fragment of LEDGF/p75 with disrupted PWWP domain and COOH terminus in HepG2 tumor cells did not affect viability under normal growth conditions but sensitized cells to serum starvation–induced death, which is known to be mediated by oxidative stress (30, 59).

The retention of intronic sequences during alternative splicing is also known to contribute to functional diversity among spliced variants (60). Our data suggest that the intron-derived COOH-terminal tail sequence (amino acids 326-333) in p52, retained in all the PWWP deletion mutants, may contribute to its proapoptotic properties but is not essential because its deletion failed to completely reduce the number of transfected cells with apoptotic nuclei. The mechanism by which the COOH-terminal tail may contribute to the proapoptotic function of p52 remains to be elucidated.

It is tempting to speculate that LEDGF splice variants may play multiple roles depending on the cell type and environment. Some of these variants may function as general transcription coactivators under normal growth conditions, in which their prosurvival or proapoptotic functions are kept in check by strict compartmentalization or by the level and type of posttranslational modifications. However, under increased oxidative stress conditions, such as those found in many tumors, these variants may

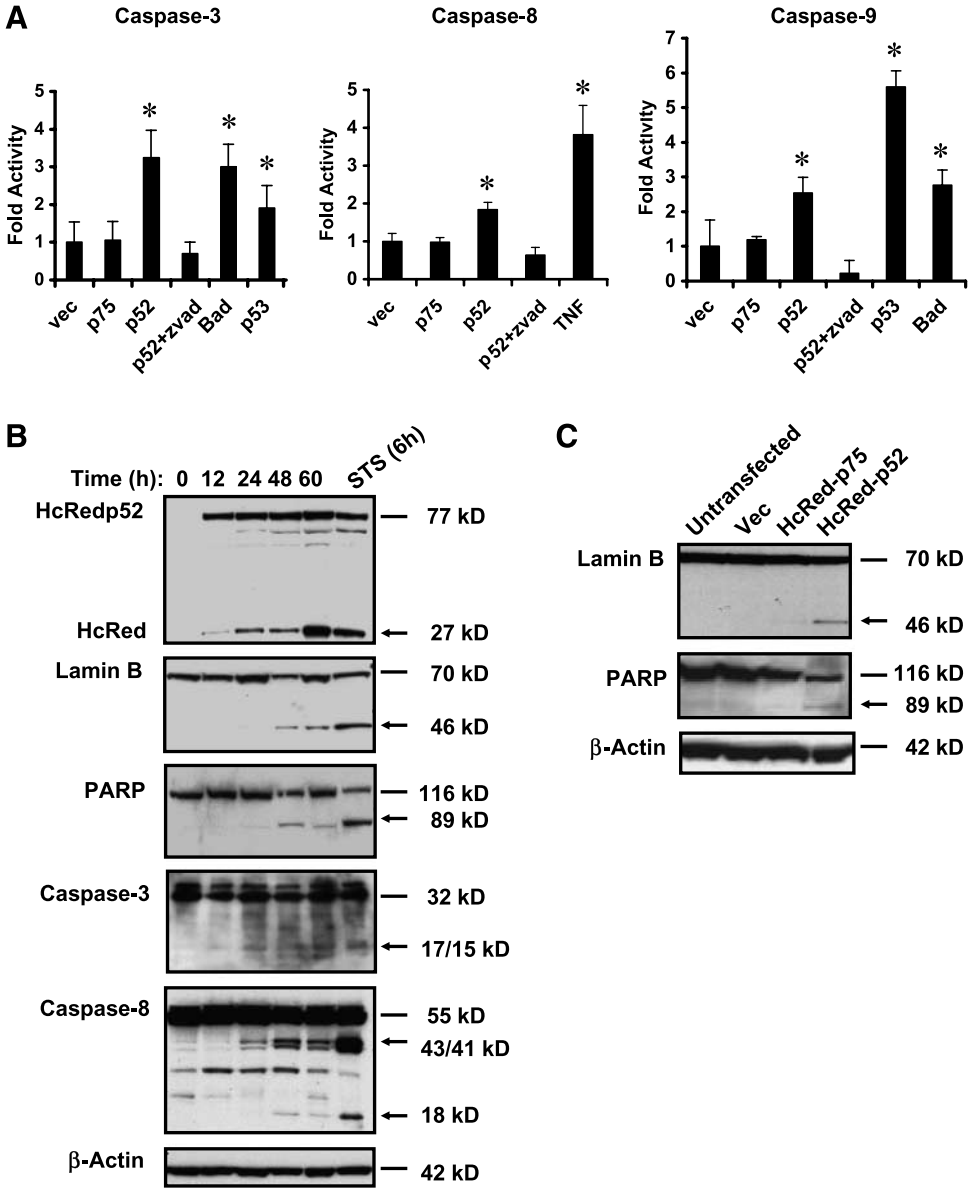

FIGURE 8. Ectopic expression of p52, but not LEDGF/p75, induces caspase activation and cleavage of prototype caspase-3 substrates. **A.** U2OS cells were transiently transfected for 48 h with empty pHcRed vector (*vec*), pHcRed-LEDGF/p75, pHcRed-p52, or the positive control plasmids pcDNA-FLAG-Bad and pcDNA-3p-p53. Treatment with TNF was also used as a control for caspase activation. Cells were also pretreated with z-VAD-fmk before transfection. Forty-eight hours after transfection, caspase activity was assayed and fold activation determined as described in Materials and Methods. Columns, mean of at least three independent experiments done in triplicate; bars, SD. *, $P < 0.05$, compared with empty pHcRed vector (one-way ANOVA, GraphPad Prism). **B.** U2OS cells were transiently transfected for up to 60 h with pHcRed-p52. Whole-cell lysates were analyzed by SDS-PAGE and immunoblotting with antibodies to HcRed, poly(ADP-ribose) polymerase, lamin B, caspase-3, caspase-8, and β-actin. **C.** U2OS cells were transiently transfected for 48 h with pHcRed-LEDGF/p75, pHcRed-p52, or empty pHcRed vector. Whole-cell lysates were analyzed by SDS-PAGE and immunoblotting with antibodies to poly (ADP-ribose) polymerase, lamin B, and β-actin. Lines, intact proteins; arrows, cleavage fragments.

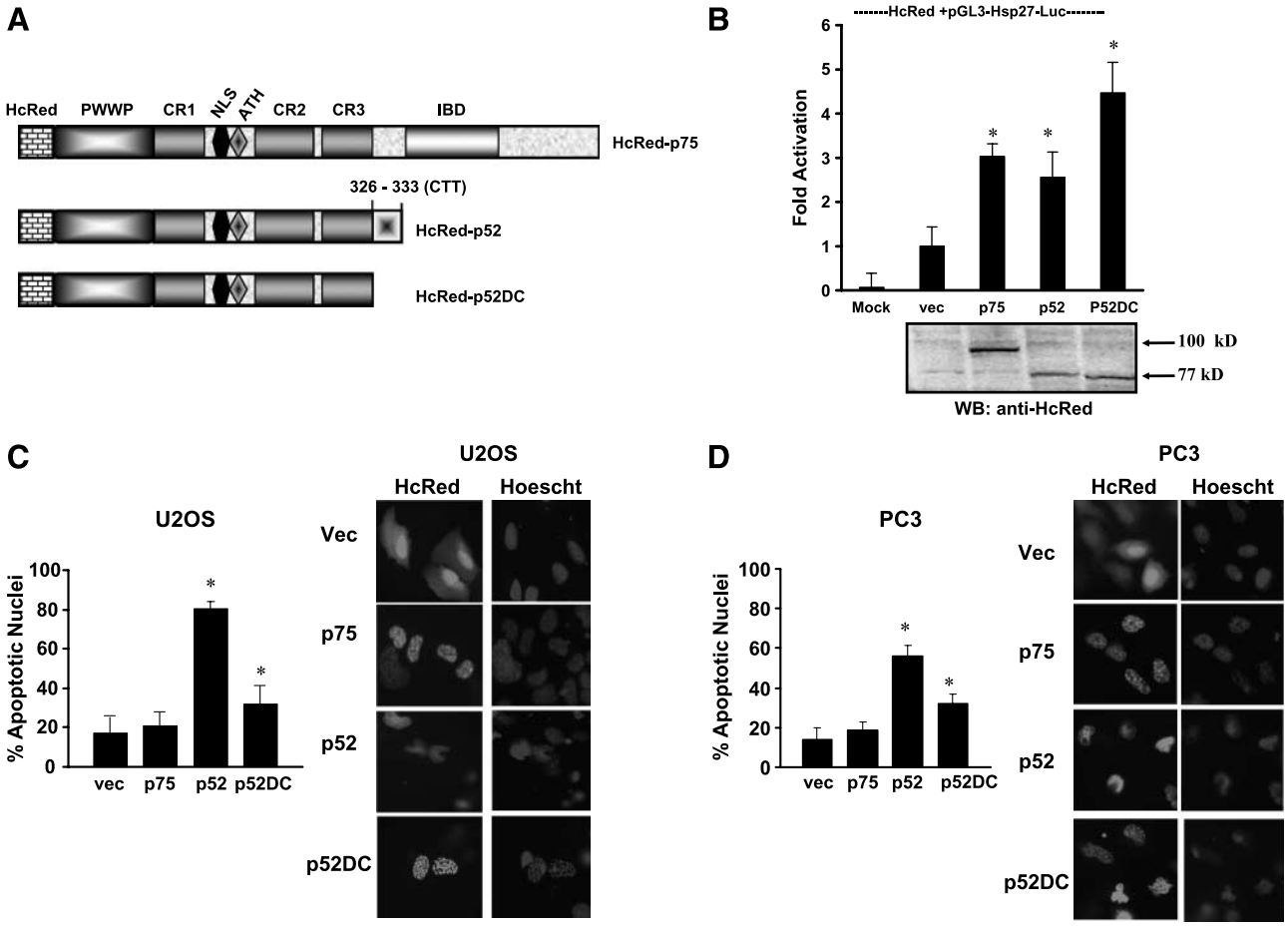

FIGURE 9. Contribution of COOH-terminal tail sequence to transcriptional potential and proapoptotic activity of p52. **A.** Schematic diagram of HcRed-LEDGF/p75, HcRed-p52, and HcRed-p52DC. **B.** HCT116 cells were cotransfected with pGL3-Hsp27pr-Luc and empty pHcRed vector, HcRed-LEDGF/p75, HcRed-p52, or HcRed-p52DC. Forty-eight hours posttransfection, cell lysates were assayed for luciferase activity or analyzed by immunoblotting with anti-HcRed antibody. Columns, mean of three independent experiments done in triplicate; bars, SD. *, $P < 0.05$, compared with empty pHcRed vector (one-way ANOVA, GraphPad). **C.** U2OS cells were transiently transfected with empty pHcRed vector, pHcRed-LEDGF/p75, pHcRed-p52, or pHcRed-p52DC. Forty-eight hours posttransfection, nuclei were counterstained with Hoechst and cells were visualized by fluorescence microscopy. The percent of apoptotic nuclei was calculated for the transfected cell populations as indicated in the legend of Fig. 7. **D.** Same as in **C** but with PC3 cells. Columns, mean of at least three independent experiments; bars, SD. *, $P < 0.05$, compared with empty pHcRed vector (one-way ANOVA, GraphPad).

antagonize each other, perhaps by competing for promoter regions or interactions with transcription factors. Their relative expression ratio might also determine whether the tumor cell response to stress shifts toward survival or death. It should be emphasized that most cancer cell lines examined in this study expressed a high p75/p52 ratio, consistent with the findings of Huang et al. (33) in leukemic cells. Whereas LEDGF/p75 is overexpressed in human cancers (30-33), its proapoptotic splice variants might be down-regulated, thus providing a survival advantage in the presence of oxidative stress or chemotherapeutic drugs. Unbalanced expression of splice isoforms in tumor cells could be caused by mutations in *cis*-acting splicing elements or by environment-driven changes in the activity of splicing proteins, which may affect tumor development and progression (60-62).

Understanding the role of LEDGF splice variants in the regulation of tumor cell death and survival under stress, combined with modulation of their expression in human tumors, may lead to novel strategies to circumvent tumor chemoresistance. Any enhancement of therapy-induced survival time will have a profound and positive effect on the lives of cancer patients and may also translate into a reduction of racial/ethnic disparities in cancer mortality.

Materials and Methods

Cells, Antibodies, and Reagents

HCT116, U2OS, HepG2, HeLa, and Jurkat cell lines were purchased from American Type Culture Collection. The 293T cell line was purchased from Orbigen. Cells were routinely maintained in either McCoy's 5A medium, DMEM, or RPMI 1640, supplemented with 10% fetal bovine serum (Omega Scientific), 1.5 mmol/L L-glutamine (Cellgro), and penicillin/streptomycin or gentamicin (Cellgro). The prostate cell lines were previously described and cultured as indicated (29). All cell lines were maintained in the presence of 5% CO_2 at 37°C.

The following antibodies were used in this study: mouse monoclonals anti-LEDGF/p75 and p52 (BD Biosciences),

anti–β-actin (Sigma), anti–poly(ADP-ribose) polymerase (R&D Systems), anti–caspase-3 (PharMingen), and anti–caspase-8 (Alexis); rabbit polyclonals anti-HA (Santa Cruz Biotechnology) and anti-HcRed (Clontech); goat anti–lamin B (Santa Cruz Biotechnology), Alexa Flour 488–conjugated goat anti-rabbit IgG (Molecular Probes), and rat monoclonal horseradish peroxidase (HRP)–conjugated anti-HA antibody (Roche Diagnostics). All other HRP-conjugated secondary antibodies were from Zymed. Rabbit anti-p52 antibody was raised against a synthetic 15-mer peptide containing the COOH-terminal tail (amino acids 318-333; Biosource International). Human autoantibodies to LEDGF/p75, topoisomerase I, and upstream binding factor were a kind gift from Dr. Eng M. Tan (Scripps Research Institute, La Jolla, CA). Human TNF-α, etoposide, cycloheximide, and 4′,6-diamidino-2-phenylindole were from Sigma-Aldrich. Hoechst 33342 was from Molecular Probes. Staurosporine and the caspase substrates Asp-Glu-Val-Asp-7-amino-4-methyl coumarin (DEVD-AMC), Ile-Glu-Thr-Asp-AMC (IETD-AMC), and Leu-Glu-His-Asp-AMC (LEHD-AMC) were from Alexis. z-VAD-fmk was from Biomol International and z-DEVD-fmk was from Enzyme Systems Products. Purified caspases were from PharMingen.

Apoptosis Assays

Apoptosis was induced in HCT116 cells with 10 ng/mL TNF-α in combination with 20 μmol/L cycloheximide. HCT116 cells were also preincubated with either 100 μmol/L z-VAD-fmk or z-DEVD-fmk for 1 h before exposure to TNF-α. Apoptosis was induced in HeLa and Jurkat cells with 2 μmol/L staurosporine and 150 μmol/L etoposide, respectively. In some experiments, cells were transiently transfected with the appropriate expression plasmids using Fugene 6 (Roche Diagnostics) or Amaxa Nucleofection (Amaxa, Inc.). The medium was removed 24 h posttransfection to discard cells killed during the transfection procedure; at 36 to 48 h posttransfection, cells were visualized under fluorescence microscopy, processed for determination of caspase activity or viability, or processed for SDS-PAGE (NuPAGE 4-12%, Invitrogen) and immunoblotting analysis. For quantification of apoptotic nuclei, cells were cultured in 35-mm dishes to ~60% to 70% confluency and transfected with plasmids encoding HcRed-fusion proteins. Thirty six to 48 h posttransfection, cells were counterstained with Hoechst 33342 and visualized directly using a 60× water immersion objective under an Olympus BX50 epifluorescence microscope (Scientific Instruments) equipped with a digital SPOT camera system (Diagnostic Instruments). Nuclei of cells expressing HcRed-tagged proteins that exhibited marked chromatin condensation, margination, or fragmentation were counted as apoptotic. Approximately 200 nuclei distributed in >10 different fields were counted in at least four independent double-blind experiments.

One-step cellular caspase activity assays were done in transfected cells cultured in 96-well plates in the presence of the appropriate caspase substrate, as previously described (63). Cell survival was determined using the standard 3-(4,5-dimethylthiazol-2-yl)-2,5-diphenyltetrazolium bromide assay (Sigma-Aldrich). All immunoblotting studies were done as previously described (30).

Immunofluorescence Microscopy

Cells seeded on coverslips and transfected with pCruzHA plasmids were fixed for 15 min at room temperature with 3.7% paraformaldehyde and permeabilized in PBS-0.2% Triton X-100 for 5 min. Coverslips were then incubated with rabbit anti-HA antibody for 2 h. Following three washes with PBS, cells were incubated with Alexa 488 goat anti-rabbit for 1 h, washed with PBS, mounted on glass slide with Vectashield Mounting Medium containing 4′,6-diamidino-2-phenylindole, and examined under a fluorescence microscope.

Reverse Transcription-PCR

Total RNA from HCT116 cells was isolated 48 h after transfection with pCruzHA empty vector, pCruzHA-p75, or pCruzHA-p52 using Fugene 6 (Roche Diagnostics). cDNA was synthesized using the Invitrogen SuperScript III first-strand cDNA synthesis system. Hsp27 forward primer (5′-GAGATCACCGGCAAGCACGAG-3′) and Hsp27 reverse primer (5′-CGGCAGTCTCATCGGATTTTGC-3′) were used to amplify Hsp-27 PCR products (255 bp). Cofilin 1 (CFL1) forward primer (5′-CCTTCCCAAACTGCTTTTGAT-3′) and CFL1 reverse primer (5′-CTGGTCCTGCTTCCATGAGTA-3′) were used to amplify cofilin PCR products (287 bp). Briefly, cDNA was added into a 50-μL reaction mixture containing 12.5 μL of PCR master mix and 500 nmol/L of primers. Reverse transcription was carried out at 50°C for 50 min, followed by incubation with RNase H at 37°C for 20 min. The PCR parameters were preheating at 94°C for 2 min, followed by 35 cycles of 94°C for 30 s, 57°C for 1 min 30 s, and 72°C for 1 min 30 s. Final elongation was at 72°C for 10 min. PCR reactions were separated on a 1.5% agarose gel and PCR products were visualized under UV light after ethidium bromide staining. Images were obtained using the Alpha Innotech imaging system.

Plasmid Constructs

A cDNA encoding p52 was amplified by PCR using pET28a-*ledgf/p75* template DNA (30) and the primers 5′-CGGAATTCATCACTCGCGATTTCAAACCTGGAG-3′ (forward) and 5′-GCAGATCTTACTGTAGATTACATGTTGTTTGGTGCTCAG-3′ (reverse). The amplified fragment was ligated directly into the *Eco*RI-*Bgl*II sites of the pCruzHA mammalian expression vector (Santa Cruz Biotech). The LEDGF/p75 cDNA was subcloned from a pcDNA3.1-*ledgf/p75* construct (30) into pCruzHA using *Eco*RI-*Not*I digestion. The cDNAs encoding NH_2-terminal truncated p52 mutants were generated by PCR using a pET28a-*ledgf/p75* template DNA; the p52 reverse primer 5′-GCAGATCTTACTGTAGATTACATGTTGTTTGGTGCTCAG-3′; and the following forward primers: 5′DN18, 5′-ACCCCATTGGCCAGCTCGAGTA-3′; 5′DN18M, 5′-ACCACATGCGCCAGCTCGAGTA-3′; 5′DN26, 5′-GCCGGGGATATCGAAGTTCCTGATGGAGCTGTAAAG-3′; 5′DN30, 5′-AGGAGCTGTAAAGCCACCCACAAAC-3; 5′DN50, 5′-AGCTTTTTTAGGACCAAAG-3′; 5′DN85, 5′-AAACAATCCAAAAGTGAAATTCTCAAGCCAACAG-3′; and 5′DN100, 5′-ACAATCAAATGCATCATCTGATG-3′. PCR products corresponding to truncated fragments of

p52 were subcloned into the *Eco*RV/*Hpa*I site of pCruzHA. The pGL3-*Hsp27pr*-Luc promoter construct was obtained by removing the *Hsp27* promoter region from a pGL2-Luc construct followed by ligation into the pGL3-Luc reporter vector using *Sma*I-*Bgl*II digestion. The plasmids pcDNA-FLAG-Bad and pcDNA-3p-p53 were a kind gift from Dr. Marina Zemskova (Loma Linda University, Loma Linda, CA).

Site-Directed Mutagenesis

Multiple rounds of PCR-based mutagenesis were done using the QuickChange Site-Directed Mutagenesis Kit (Stratagene) to substitute aspartic acids to alanines in the putative cleavage sites of p52. The pCruzHA-p52 construct was used as a template and the following primers were used to generate the HA-DEVPA and HA-WEIA constructs: 5′-CCCCATTGGCCAGCTCGAGTAGACGAAGTTCCTGCGGGAGCTGTAAAGCCACCCACAAACAAACTACCC-3′ (5′DEVPA, forward), 5′-GGGTAGTTTGTTTGTGGGTGGCTTTACAGCTCCCGCAGGAACTTCGTCTACTCGAGCGGCCAATGGGG-3′ (3′DEVPA, reverse), 5′-GGCAAACCAAATAAAAGAAAAGGTTTTAATGAAGGTTTATGGGAGGCGGCGGGCGGCCCAAAGTGAAATTTTCAAGTCAACAGGCAGC-3′ (5′WEIA, forward), and 5′-GCTGCCTGTTGACTTGAAAATTTCACTTTTGGGCCGCCCGCCGCCTCCCATAAACCTTCATTAAAACCTTTTCTTTTATTTGGTTTGCC-3′ (3′WEIA, reverse). For the generation of the pCruzHA-*p52DM* construct, the pCruzHA-p52WEIA template and the p52DEVPA primer pairs were used. The pHcRed-p52DC construct was generated by inserting a stop codon at amino acid position 326 within the p52 nucleotide sequence. For this, pHcRed-p52 was used as template with the following primers: 5′-CGCAAGCAAGAGGAACAAATGGAAACTGAGTAGCAAGCAACGCGCAATCTACAGTAAGATCTAGAGGGCCC-3 (forward) and 5′-GGGCCCTCTAGATCTTACTGTAGATTGCGCGTTGCTTGCTACTCAGTTTCCATTTGTTCCTCTTGCTTGCG-3′ (reverse).

In vitro *Transcription/Translation*

cDNAs were transcribed and translated *in vitro* using the TNT T7 Coupled Reticulocyte Lysate System and Transcend Non-Radioactive Translation Detection System (Promega) at 30°C for 90 min as indicated previously (30). Using these systems, biotinylated lysine was added to the transcription-translation reaction as a precharged epsilon-labeled biotinylated lysine-tRNA complex (provided by the manufacturer). Biotinylated translated proteins were incubated with caspase cleavage buffer [100 mmol/L NaCl, 20 mmol/L PIPES (pH 7.2), 1 mmol/L EDTA, 10% sucrose, 0.1% CHAPS, 100 mmol/L DTT] with or without purified caspases. Biotinylated translated proteins were separated by SDS-PAGE, transferred to nitrocellulose, and detected with HRP-streptavidin and enhanced chemiluminescence (Perkin-Elmer).

Luciferase-Based Transcription Reporter Assays

HCT116 or U2OS cells were cotransfected with plasmid constructs encoding the proteins of interest and pGL3 basic luciferase reporter plasmids, with or without the *Hsp27pr*. At 48 h posttransfection, cells were lysed in reporter lysis buffer and luciferase assays were done using the Luciferase Assay System (Promega). The assays were done in opaque luminometer-compatible microplates and relative light units were obtained in a MicroLumatPlus Lb 96V luminometer (Berthold Tech). Luciferase values were normalized to the amount of protein in each sample, and fold induction was calculated by normalizing to the luciferase activity in lysates from cells cotransfected with the empty vectors (pCruzHA, pcDNA3.1+, or pHcRed) and pGL3-*Hsp27pr*-Luc or pGL3-Luc.

Chromatin Fractionation

Chromatin fractionation was done essentially as described previously (64). Briefly, cells transiently transfected with different plasmid constructs were collected after trypsinization, washed twice with PBS (2 min, 1,700 × g, 4°C), and resuspended in 200 μL of buffer A [10 mmol/L HEPES (pH 7.9), 10 mmol/L KCl, 1.5 mmol/L $MgCl_2$, 0.34 mol/L sucrose, 10% glycerol, 1 mmol/L DTT, 0.5 μg/mL of pepstatin A, and protease inhibitor cocktail]. This cell suspension was treated with Triton X-100 (0.1% final concentration) and incubated on ice for 8 min; the nuclei were collected by centrifugation (5 min, 1,300 × *g*, 4°C). The supernatant was further centrifuged (5 min, 20,000 × *g*, 4°C) and the resulting supernatant, called soluble fraction, was collected. The nuclear fraction was washed once in 200-μL buffer A and lysed for 30 min in 100-μL buffer B (3 mmol/L EDTA, 0.2 mmol/L EGTA, 1 mmol/L DTT, 0.5 μg/mL of pepstatin A, and protease inhibitor cocktail). The insoluble chromatin fraction was collected by centrifugation (5 min, 1,700 × *g*, 4°C) and washed once with buffer B. Fractions were mixed with SDS sample buffer and boiled for 10 min. Proteins were then separated by SDS-PAGE and analyzed by immunoblotting.

Disclosure of Potential Conflicts of Interest

No potential conflicts of interest were disclosed.

Acknowledgments

We thank the following colleagues from Loma Linda University School of Medicine for valuable discussions and suggestions and for technical advice: Marino De Leon, Penny Duerksen-Hughes, Hansel Fletcher, Mark Johnson, Michael B. Lilly, and Marina Zemskova.

References

1. Borek C. Dietary antioxidants and human cancer. Integr Cancer Ther 2004;3:333–41.

2. Pathak SK, Sharma RA, Steward WP, Mellon JK, Griffiths TR, Gescher AJ. Oxidative stress and cyclooxygenase activity in prostate carcinogenesis: targets for chemopreventive strategies. Eur J Cancer 2005;41:61–70.

3. Robertson RP, Harmon JS. Diabetes, glucose toxicity, and oxidative stress: A case of double jeopardy for the pancreatic islet beta cell. Free Radic Biol Med 2006;41:177–84.

4. Giles GI. The redox regulation of thiol dependent signaling pathways in cancer. Curr Pharm Des 2006;12:4427–43.

5. Kinnula VL, Paakko P, Soini Y. Antioxidant enzymes and redox regulating thiol proteins in malignancies of human lung. FEBS Lett 2004;569:1–6.

6. Pennington JD, Wang TJ, Nguyen P, Sun L, Bisht K, Smart D, Gius D. Redox-sensitive signaling factors as novel molecular targets for cancer therapy. Drug Resist Updat 2005;8:322–30.

7. Ganapathy V, Daniels T, Casiano CA. LEDGF/p75: a novel nuclear autoantigen at the crossroads of cell survival and apoptosis. Autoimmun Rev 2003;2:290–7.

8. Shinohara T, Singh DP and Fatma N. LEDGF, a survival factor, activates stress-related genes. Prog Retin Eye Res 2002;21:341–58.

9. Takamura Y, Fatma N, Kubo E, Singh DP. Regulation of heavy subunit chain of γ-glutamylcysteine synthetase by tumor necrosis factor-α in lens epithelial cells: role of LEDGF/p75. Am J Physiol Cell Physiol 2006;290: C554–66.

10. Ge H, Si Y, Roeder RG. Isolation of cDNAs encoding novel transcription coactivators p52 and p75 reveals an alternate regulatory mechanism of transcriptional activation. EMBO J 1998;17:6723–9.

11. Ochs RL, Muro Y, Si Y, Ge H, Chan EK, Tan EM. Autoantibodies to DFS 70 kd/transcription coactivator p75 in atopic dermatitis and other conditions. J Allergy Clin Immunol 2000;105:1211–20.

12. Sutherland HG, Newton K, Brownstein DG, et al. Disruption of Ledgf/Psip1 results in perinatal mortality and homeotic skeletal transformations. Mol Cell Biol 2006;26:7201–10.

13. Fatma N, Singh DP, Shinohara T, Chrylack LT, Jr. Transcriptional regulation of the antioxidant protein 2 gene, a thiol-specific antioxidant, by lens epithelium-derived growth factor to protect cells from oxidative stress. J Biol Chem 2001; 276:48899–907.

14. Fatma N, Kubo E, Chylack LT, Jr., Shinohara T, Akagi Y, Singh DP. LEDGF regulation of alcohol and aldehyde dehydrogenases in lens epithelial cells: stimulation of retinoic acid production and protection from ethanol toxicity. Am J Physiol Cell Physiol 2004;287:C508–16.

15. Sharma P, Singh DP, Fatma N, Chylack LT, Jr., Shinohara T. Activation of LEDGF gene by thermal-and oxidative-stresses. Biochem Biophys Res Commun 2000;276:1320–4.

16. Singh DP, Fatma N, Kimura A, Chylack LT, Jr., Shinohara T. LEDGF binds to heat shock and stress-related element to activate the expression of stress-related genes. Biochem Biophys Res Commun 2001;283:943–55.

17. Dellavance A, Viana VS, Leon EP, Bonfa ES, Andrade LE, Leser PG. The clinical spectrum of antinuclear antibodies associated with the nuclear dense fine speckled immunofluorescence pattern. J Rheumatol 2005;32: 2144–9.

18. Ganapathy V, Casiano CA. Autoimmunity to the nuclear autoantigen DFS70 (LEDGF): what exactly are the autoantibodies trying to tell us? Arthritis Rheum 2004;50:684–8.

19. Muro Y, Ogawa Y, Sugiura K, Tomita Y. HLA-associated production of anti-DFS70/LEDGF autoantibodies and systemic autoimmune disease. J Autoimmun 2006;26:252–7.

20. Ciuffi A, Bushman FD. Retroviral DNA integration: HIV and the role of LEDGF/p75. Trends Genet 2006;22:388–95.

21. Hombrouck A, De Rijck J, Hendrix J, et al. Virus evolution reveals an exclusive role for LEDGF/p75 in chromosomal tethering of HIV. PLoS Pathog 2007;3:e47.

22. Van Maele B, Busschots K, Vandekerckhove L, Christ F, Debyser Z. Cellular co-factors of HIV-1 integration. Trends Biochem Sci 2006;31: 98–105.

23. Shun MC, Raghavendra NK, Vandegraaff N, et al. LEDGF/p75 functions downstream from preintegration complex formation to effect gene-specific HIV-1 integration. Genes Dev 2007;21:1767–78.

24. Marshall HM, Ronen K, Berry C, et al. Role of PSIP1/LEDGF/p75 in lentiviral infectivity and integration targeting. PLoS ONE 2007;2: e1340.

25. Dietz F, Franken S, Yoshida K, Nakamura H, Kappler J, Gieselmann V. The family of hepatoma-derived growth factor proteins: characterization of a new member HRP-4 and classification of its subfamilies. Biochem J 2002;366: 491–500.

26. Ahuja HG, Hong J, Aplan PD, Tcheurekdjian L, Forman SY, Slovak ML. t(9;11)(p22;p15) in acute myeloid leukemia results in a fusion between NUP98 and the gene encoding transcriptional coactivators p52 and p75-lens epithelium-derived growth factor (LEDGF). Cancer Res 2000;60: 6227–9.

27. Grand FH, Koduru P, Cross NC, Allen SL. NUP98-LEDGF fusion and t(9;11) in transformed chronic myeloid leukemia. Leuk Res 2005;29: 1469–72.

28. Hussey DJ, Moore S, Nicola M, Dobrovic A. Fusion of the NUP98 gene with the LEDGF/p52 gene defines a recurrent acute myeloid leukemia translocation. BMC Genet 2001;2:20.

29. Morerio C, Acquila M, Rosanda C, et al. t(9;11)(p22;p15) with NUP98-LEDGF fusion gene in pediatric acute myeloid leukemia. Leuk Res 2005;29: 467–70.

30. Wu X, Daniels T, Molinaro C, Lilly MB, Casiano CA. Caspase cleavage of the nuclear autoantigen LEDGF/p75 abrogates its pro-survival function: implications for autoimmunity in atopic disorders. Cell Death Differ 2002;9: 915–25.

31. Daniels T, Zhang J, Gutierrez I, et al. Antinuclear autoantibodies in prostate cancer: immunity to LEDGF/p75, a survival protein highly expressed in prostate tumors and cleaved during apoptosis. Prostate 2005;62: 14–26.

32. Daugaard M, Kirkegaard-Sorensen T, Ostenfeld MS, et al. Lens epithelium-derived growth factor is an Hsp70-2 regulated guardian of lysosomal stability in human cancer. Cancer Res 2007;67:2559–67.

33. Huang TS, Myklebust LM, Kjarland E, et al. LEDGF/p75 has increased expression in blasts from chemotherapy-resistant human acute myelogenic leukemia patients and protects leukemia cells from apoptosis *in vitro*. Mol Cancer 2007;6:31.

34. Singh DP, Kimura A, Chylack LT, Jr. Shinohara T. Lens epithelium-derived growth factor (LEDGF/p75) and p52 are derived from a single gene by alternative splicing. Gene 2000;242:265–73.

35. Ge H, Si Y, Wolffe AP. A novel transcriptional coactivator, p52, functionally interacts with the essential splicing factor ASF/SF2. Mol Cell 1998;2: 751–9.

36. Ge YZ, Pu MT, Gowher H, et al. Chromatin targeting of *de novo* DNA methyltransferases by the PWWP domain. J Biol Chem 2004;279: 25447–54.

37. Chen T, Tsujimoto N, Li E. The PWWP domain of Dnmt3a and Dnmt3b is required for directing DNA methylation to the major satellite repeats at pericentric heterochromatin. Mol Cell Biol 2004;24:9048–58.

38. Lukasik SM, Cierpicki T, Borloz M, Grembecka J, Everett A, Bushweller JH. High resolution structure of the HDGF PWWP domain: a potential DNA binding domain. Protein Sci 2006;15:314–23.

39. Nameki N, Tochio N, Koshiba S, et al. Solution structure of the PWWP domain of the hepatoma-derived growth factor family. Protein Sci 2005;14: 756–64.

40. Qiu C, Sawada K, Zhang X, Cheng X. The PWWP domain of mammalian DNA methyltransferase Dnmt3b defines a new family of DNA-binding folds. Nat Struct Biol 2002;9:217–24.

41. Llano M, Vanegas M, Hutchins N, Thompson D, Delgado S, Poeschla EM. Identification and characterization of the chromatin-binding domains of the HIV-1 integrase interactor LEDGF/p75. J Mol Biol 2006;360:760–73.

42. Turlure F, Maertens G, Rahman S, Cherepanov P, Engelman A. A tripartite DNA-binding element, comprised of the nuclear localization signal and two AT-hook motifs, mediates the association of LEDGF/p75 with chromatin *in vivo*. Nucleic Acids Res 2006;34:1653–75.

43. Cheperanov P, Devroe E, Silver PA, Engelman A. Identification of an evolutionarily conserved domain in human lens epithelium-derived growth factor/transcriptional co-activator p75 (LEDGF/p75) that binds HIV-1 integrase. J Biol Chem 2004;279:48883–92.

44. Ogawa Y, Sugiura K, Watanabe A, et al. Autoantigenicity of DFS70 is restricted to the conformational epitope of C-terminal α-helical domain. J Autoimmun 2004;23:221–31.

45. Vanegas M, Llano M, Delgado S, Thompson D, Peretz M, Poeschla E. Identification of the LEDGF/p75 HIV-1 integrase-interaction domain and NLS reveals NLS-independent chromatin tethering. J Cell Sci 2005;118: 1733–43.

46. Singh DP, Kubo E, Takamura Y, et al. DNA binding domains and nuclear localization signal of LEDGF: contribution of two helix-turn-helix (HTH)-like domains and a stretch of 58 amino acids of the N-terminal to the trans-activation potential of LEDGF. J Mol Biol 2006;355:379–94.

47. Schwerk C, Schulze-Osthoff K. Regulation of apoptosis by alternative pre-mRNA splicing. Mol Cell 2005;19:1–13.

48. Venables JP. Unbalanced alternative splicing and its significance in cancer. Bioessays 2006;28:378–86.

49. Fischer U, Janicke RU, Schulze-Osthoff K. Many cuts to ruin: a comprehensive update of caspase substrates. Cell Death Differ 2003;10:76–100.

50. Jacobsen LB, Calvin SA, Colvin KE, Wright M. FuGENE 6 Transfection Reagent: the gentle power. Methods 2004;33:104–12.

51. Mediavilla-Varela M, Leoh LS, Basu A, Ganapathy V, Casiano CA. LEDGFp75/DFS70, a stress response autoantigen with multiple functions and broad clinical relevance. In: Conrad K Chan, EKL, Fritzler MJ. Sack U, Shoenfeld Y, Wiik A (eds), From Etiopathogenesis to the Prediction of

Autoimmune Diseases: Relevance of Autoantibodies. Autoantigens, Autoantibodies and Autoimmunity series. Vol. 5. Lengerich (Germany) PABS Science Publishers. 2007 p.146–65.

52. Kim SM, Kee HJ, Choe N, et al. The histone methyltransferase activity of WHISTLE is important for the induction of apoptosis and HDAC1-mediated transcriptional repression. Exp Cell Res 2007;313:975–83.

53. Botbol Y, Raghavendra NK, Rahman S, Engelman A, Lavigne M. Chromatinized templates reveal the requirement for the LEDGF/p75 PWWP domain during HIV-1 integration *in vitro*. Nucleic Acids Res 2008;36:1237–46.

54. Charvet C, Alberti I, Luciano F, et al. Proteolytic regulation of Forkhead transcription factor FOXO3a by caspase-3-like proteases. Oncogene 2003;22: 4557–68.

55. Kim W, Kook S, Kim DJ, Teodorof C, Song WK. The 31-kDa caspase-generated cleavage product of p130cas functions as a transcriptional repressor of E2A in apoptotic cells. J Biol Chem 2004;279:8333–42.

56. Steinhusen U, Badock V, Bauer A, et al. Apoptosis-induced cleavage of β-catenin by caspase-3 results in proteolytic fragments with reduced transactivation potential. J Biol Chem 2000;275:16345–53.

57. Schembri L, Dalibart R, Tomasello F, Legembre P, Ichas F, De Giorgi F. The HA tag is cleaved and loses immunoreactivity during apoptosis. Nat Methods 2007;4:107–8.

58. Nishizawa Y, Usukura J, Singh DP, Chylack LT, Shinohara T. Spatial and temporal dynamics of two alternatively spliced regulatory factors, lens epithelium-derived growth factor (ledgf/p75) and p52, in the nucleus. Cell Tissue Res 2001;305:107–14.

59. Kang S, Song J, Kang H, Kim S, Lee Y, Park D. Insulin can block apoptosis by decreasing oxidative stress via phosphatidylinositol 3-kinase- and extracellular signal-regulated protein kinase-dependent signaling pathways in HepG2 cells. Eur J Endocrinol 2003;148:147–55.

60. Srebrow A, Kornblihtt AR. The connection between splicing and cancer. J Cell Sci 2006;119:2635–41.

61. Wu JY, Tang H, Havlioglu N. Alternative pre-mRNA splicing and regulation of programmed cell death. Prog Mol Subcell Biol 2003;31:153–85.

62. Ebihara K, Masuhiro Y, Kitamoto T, et al. Intron retention generates a novel isoform of the murine vitamin D receptor that acts in a dominant negative way on the vitamin D signaling pathway. Mol Cell Biol 1996;16: 3393–400.

63. Carrasco RA, Stamm NB, Patel BK. One-step cellular caspase-3/7 assay. Biotechniques 2003;34:1064–7.

64. Wysocka J, Reilly PT, Herr W. Loss of HCF-1-chromatin association precedes temperature-induced growth arrest of tsBN67 cells. Mol Cell Biol 2001; 21:3820–9.